



Asymmetric dispersal in the multi-patch logistic equation

Roger Arditi, Claude Lobry, Tewfik Sari

► To cite this version:

Roger Arditi, Claude Lobry, Tewfik Sari. Asymmetric dispersal in the multi-patch logistic equation. Theoretical Population Biology, 2018, 120, pp.11 - 15. 10.1016/j.tpb.2017.12.006 . hal-01688305

HAL Id: hal-01688305

<https://hal.sorbonne-universite.fr/hal-01688305>

Submitted on 19 Jan 2018

HAL is a multi-disciplinary open access archive for the deposit and dissemination of scientific research documents, whether they are published or not. The documents may come from teaching and research institutions in France or abroad, or from public or private research centers.

L'archive ouverte pluridisciplinaire **HAL**, est destinée au dépôt et à la diffusion de documents scientifiques de niveau recherche, publiés ou non, émanant des établissements d'enseignement et de recherche français ou étrangers, des laboratoires publics ou privés.

Asymmetric dispersal in the multi-patch logistic equation

Roger Arditi^{a,b,*}, Claude Lobry^c, Tewfik Sari^{d,e}

^aUniversity of Fribourg, Department of Biology, Chemin du Musée 10, 1700 Fribourg, Switzerland. E-mail: roger.arditi@unifr.ch

^bSorbonne Université, Institute of Ecology and Environmental Sciences (iEES-Paris), 75252 Paris cedex 05, France

^cUniversité Nice-Sophia-Antipolis, Centre de recherches en histoire des idées (CRHI), 98 boulevard Édouard Herriot, BP 3209, 06204 Nice cedex, France. E-mail: lobrinria@wanadoo.fr

^dITAP, Irstea, Montpellier SupAgro, Univ Montpellier, Montpellier, France. E-mail: tewfik.sari@irstea.fr

^eUniversité de Haute Alsace, LMIA, Mulhouse, France

*Corresponding author

Key words: Fragmented habitat; migration rate; logistic growth; carrying capacity

December 19, 2017

Abstract

The standard model for the dynamics of a fragmented density-dependent population is built from several local logistic models coupled by migrations. First introduced in the 1970s and used in innumerable articles, this standard model applied to a two-patch situation has never been fully analyzed. Here, we complete this analysis and we delineate the conditions under which fragmentation associated with dispersal is either favorable or unfavorable to total population abundance. We pay special attention to the case of asymmetric dispersal, i.e., the situation in which the dispersal rate from patch 1 to patch 2 is not equal to the dispersal rate from patch 2 to patch 1. We show that this asymmetry can have a crucial quantitative influence on the effect of dispersal.

1 Introduction

- 2 We deal here with population dynamics of a fragmented population. This is a problem
- 3 with potentially very important applied aspects. For example, in conservation ecology,
- 4 a standard question is whether a single large refuge is better or worse than several

5 small ones, with the objective of maximizing the total population abundance of an
6 endangered species (the SLOSS debate; see, e.g., Hanski, 1999). On the contrary,
7 in the context of pest control, the question is whether a single large field is better or
8 worse than several small ones, with the objective of minimizing the occurrence of an
9 insect pest or a plant disease. A huge body of theoretical literature exists around these
10 questions. However, even the simplest and most ancient model still contains unresolved
11 aspects with unsupported generalizations.

12 The theoretical paradigm that has been used to treat these questions is that of a
13 single population fragmented into two coupled patches. It is widely accepted to as-
14 sume that each subpopulation in each patch follows a local logistic law and that the
15 two patches are coupled by density-independent migrations. Freedman and Waltman
16 (1977) were first to propose the following model:

$$\begin{cases} \frac{dN_1}{dt} &= r_1 N_1 \left(1 - \frac{N_1}{K_1}\right) + \beta (N_2 - N_1), \\ \frac{dN_2}{dt} &= r_2 N_2 \left(1 - \frac{N_2}{K_2}\right) + \beta (N_1 - N_2), \end{cases} \quad (1)$$

17 where N_i is the population abundance in patch i . The parameters r_i and K_i are re-
18 spectively the intrinsic growth rate and the carrying capacity in patch i and β is the
19 migration rate, assumed to be identical in both directions. All parameters are assumed
20 to be positive.

21 After Freedman and Waltman (1977), aspects of this model were later studied by
22 DeAngelis et al. (1979) and Holt (1985), and a graphical presentation was given by
23 Hanski (1999, pp. 43–46) in his reference book on metapopulations. More recently,
24 DeAngelis and Zhang (2014), DeAngelis et al. (2016) have brought new developments.
25 We think we were first to publish the full mathematical study of model (1) in Arditi et
26 al. (2015).

27 A limitation of model (1) is the assumption of symmetric dispersal: the single
28 parameter β quantifies the migration rate from patch 1 to patch 2 and from patch 2 to
29 patch 1. In the present paper, we will expand our first analysis to the case of asymmetric
30 dispersal between patches and we will delineate the conditions under which dispersal
31 can either be favorable or unfavorable to total population abundance.

32 We denote by N_1^* and N_2^* the population abundances at equilibrium. In isolation
33 ($\beta = 0$), each population equilibrates at its local carrying capacity: $N_i^* = K_i$. Freedman
34 and Waltman (1977) analyzed the model in the case of perfect mixing ($\beta \rightarrow \infty$) and
35 showed that the total equilibrium population, $N_T^* = N_1^* + N_2^*$, is generally different from
36 the sum of the carrying capacities $K_1 + K_2$. Depending on the parameters, N_T^* can either
37 be greater or smaller than $K_1 + K_2$. For instance, if $r_1/K_1 < r_2/K_2$ (with $K_1 < K_2$), we
38 will have $N_T^* > K_1 + K_2$, which means that dispersal is favorable with respect to the
39 total equilibrium population. This spectacular result, somewhat paradoxical, has been
40 widely discussed and has led to speculations about the general virtues of patchiness
41 and dispersal.

42 Freedman and Waltman (1977) only contrasted the situations of perfect isolation
43 and perfect mixing; they did not study the effect of intermediate values of the dispersal
44 parameter β . This effect was studied by DeAngelis and Zhang (2014), but only in the
45 special case $r_1/K_1 = r_2/K_2$. In our earlier paper (Arditi et al. 2015), we calculated

the full set of parameter conditions for which dispersal is favorable or not to total population abundance.

In another paper, Arditi et al. (2016) returned to the simpler case of perfect mixing (i.e., with the migration rate $\beta \rightarrow \infty$) in order to compare the properties of Verhulst's and Lotka's formulations of the logistic model in relation with the paradox outlined above (the non-additivity of carrying capacities). In a criticism of this paper, Ramos-Jiliberto and Moisset de Espanés (2017) proposed the following alternative model:

$$\begin{cases} \frac{dN_1}{dt} &= r_1 N_1 \left(1 - \frac{N_1}{K_1}\right) + \beta \left(\frac{N_2}{K_2} - \frac{N_1}{K_1}\right), \\ \frac{dN_2}{dt} &= r_2 N_2 \left(1 - \frac{N_2}{K_2}\right) + \beta \left(\frac{N_1}{K_1} - \frac{N_2}{K_2}\right). \end{cases} \quad (2)$$

In this model, the dispersal rate is β/K_i . It is different in each direction: the probability of an individual to leave its patch is inversely proportional to the local carrying capacity. This is known as the Balanced Dispersal Model proposed by McPeck and Holt (1992). Ramos-Jiliberto and Moisset de Espanés (2017) showed that, in this model, the equality $N_T^* = K_1 + K_2$ is always true. Thus, the model (2) does not present the "perfect mixing paradox": there is strict additivity of carrying capacities.

In their reply to Ramos-Jiliberto and Moisset de Espanés (2017), Arditi et al. (2017) moved beyond the polemical opposition of models (1) and (2) by embedding both of them into the following more general model with differential dispersal:

$$\begin{cases} \frac{dN_1}{dt} &= r_1 N_1 \left(1 - \frac{N_1}{K_1}\right) + \beta \left(\frac{N_2}{\gamma_2} - \frac{N_1}{\gamma_1}\right), \\ \frac{dN_2}{dt} &= r_2 N_2 \left(1 - \frac{N_2}{K_2}\right) + \beta \left(\frac{N_1}{\gamma_1} - \frac{N_2}{\gamma_2}\right). \end{cases} \quad (3)$$

As in model (2), the dispersal rate (β/γ_i) is generally different in each direction. However, this model encompasses both (1) and (2) because model (1) corresponds to the case $\gamma_1 = \gamma_2 = 1$ and model (2) corresponds to the case $\gamma_1 = K_1$, $\gamma_2 = K_2$. Note that model (3) is overparameterized in order that it can be written in a symmetric way. Among the parameters β , γ_1 , and γ_2 , two only are independent. With no loss of generality, the ratio γ_2/γ_1 can be considered as a single parameter. Thus, model (3)'s total number of independent parameters is six, not seven. In this parameterization, β quantifies the migration intensity and γ_2/γ_1 quantifies the migration asymmetry.

Assuming perfect mixing (i.e., $\beta \rightarrow \infty$), Arditi et al. (2017) showed that the paradox exhibited by model (1) is a generic property of the more general model (3). They showed that its absence in model (2) corresponds to a very special case in parameter space, i.e., balanced dispersal. They also showed that a second special case exists for which carrying capacity additivity is observed.

The purpose of the present paper is to perform the mathematical analysis of the general model (3) in the full parameter space. That is, we will consider all finite positive values of β and no longer assume perfect mixing as in Arditi et al. (2017).

78 2 Equilibrium analysis

79 The equilibria of the dynamic model (3) are the solutions of the algebraic system

$$\begin{cases} 0 &= r_1 N_1 \left(1 - \frac{N_1}{K_1}\right) + \beta \left(\frac{N_2}{\gamma_2} - \frac{N_1}{\gamma_1}\right), \\ 0 &= r_2 N_2 \left(1 - \frac{N_2}{K_2}\right) + \beta \left(\frac{N_2}{\gamma_2} - \frac{N_1}{\gamma_1}\right). \end{cases} \quad (4)$$

80 Adding the two equations gives

$$r_1 N_1 \left(1 - \frac{N_1}{K_1}\right) + r_2 N_2 \left(1 - \frac{N_2}{K_2}\right) = 0, \quad (5)$$

81 which is the equation of an ellipse (shown in red in Fig. 1 and the other figures). This
 82 ellipse \mathcal{E} passes through the points $(0, 0)$, $(K_1, 0)$, $(0, K_2)$, and (K_1, K_2) . It does not
 83 depend on the migration intensity β (or on the migration asymmetry γ_2/γ_1).

84 Solving the first equation in (4) for N_2 yields a parabola \mathcal{P}_β of equation $N_2 =$
 85 $P_\beta(N_1)$, where the function P_β is defined by

$$P_\beta(N_1) = \gamma_2 \left(\frac{N_1}{\gamma_1} - \frac{r_1}{\beta} N_1 \left(1 - \frac{N_1}{K_1}\right) \right). \quad (6)$$

86 This parabola \mathcal{P}_β (shown in blue in Fig. 1 and the other figures) depends on the
 87 migration intensity β (and on γ_2/γ_1). It always passes through the points 0 and $\Omega =$
 88 $(K_1, K_1 \gamma_2/\gamma_1)$.

The equilibria are the nonnegative intersections of the ellipse \mathcal{E} and the parabola \mathcal{P}_β . There are two equilibrium points. The first is the trivial point $(0, 0)$ and the second is a nontrivial point whose position depends on β :

$$E_\beta = (N_{1\beta}^*, N_{2\beta}^*).$$

89 A straightforward isocline analysis (see Fig. 2) shows that $(0, 0)$ is always unstable
 90 and that E_β is always stable.

91 When $\beta \rightarrow 0$, the left branch of the parabola \mathcal{P}_β merges into the vertical line $N_1 = 0$
 92 and the right branch into the vertical line $N_1 = K_1$ (\mathcal{P}_0 in Fig. 1). The parabola's limit
 93 for $\beta \rightarrow \infty$ is the oblique line $N_2 = (\gamma_2/\gamma_1)N_1$ (\mathcal{P}_∞ in Fig. 1).

94 We denote by A the intersection of the ellipse \mathcal{E} with \mathcal{P}_0 and by B the intersection
 95 of \mathcal{E} with \mathcal{P}_∞ . $A = (K_1, K_2)$ is the perfect-isolation equilibrium and B is the perfect-
 96 mixing equilibrium. It is easy to calculate that

$$B = (B_1, B_2) = \left(\frac{(\gamma_1/\gamma_2)r_1 + r_2}{(\gamma_1/\gamma_2)r_1/K_1 + (\gamma_2/\gamma_1)r_2/K_2}, \frac{r_1 + (\gamma_2/\gamma_1)r_2}{(\gamma_1/\gamma_2)r_1/K_1 + (\gamma_2/\gamma_1)r_2/K_2} \right). \quad (7)$$

97 The slope of \mathcal{P}_∞ is B_2/B_1 . With the expressions in (7), this slope is found to be
 98 γ_2/γ_1 . As this ratio can vary from 0 to ∞ , B can be anywhere on the ellipse \mathcal{E} in the
 99 positive quadrant. As β increases from 0 to ∞ , the equilibrium point E_β follows the
 100 ellipse arc from A to B . This change is clockwise if $\gamma_2/\gamma_1 < K_2/K_1$ or counterclockwise
 101 if $\gamma_2/\gamma_1 > K_2/K_1$ (respectively left and right panels of Fig. 1).

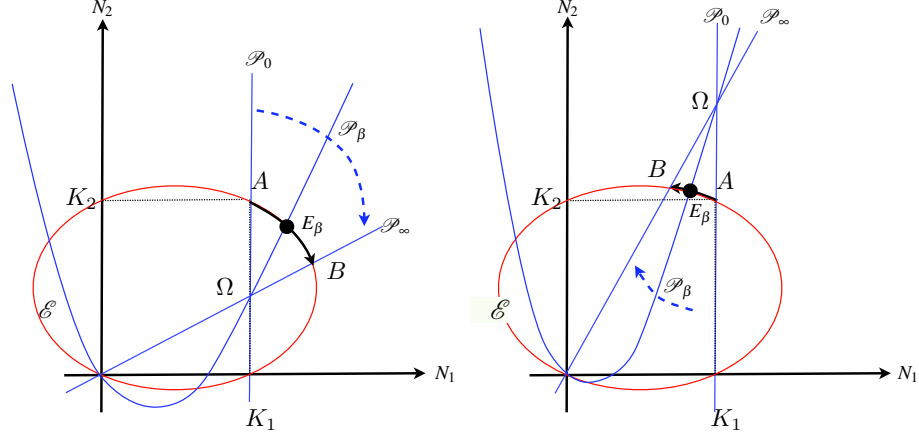


Figure 1: The equilibrium point E_β is the positive intersection of the ellipse \mathcal{E} and the parabola \mathcal{P}_β . The lines \mathcal{P}_0 and \mathcal{P}_∞ are the limits of \mathcal{P}_β for $\beta = 0$ and for $\beta \rightarrow \infty$. The slope of \mathcal{P}_∞ is γ_2/γ_1 . The equilibrium E_β can only belong to the ellipse arc between A and B. Left: $\gamma_2/\gamma_1 < K_2/K_1$. Right: $\gamma_2/\gamma_1 > K_2/K_1$.

102 In the special case $\gamma_2/\gamma_1 = K_2/K_1$, the points A and B become confounded and
 103 the equilibrium E_β does not depend on β ; it is always equal to (K_1, K_2) and thus $N_T^* =$
 104 $K_1 + K_2$. This is the special case considered by Ramos-Jiliberto and Moisset de Espanés
 105 (2017). Note that this occurs in wider conditions than those assumed by these authors:
 106 β can have any value, not only $\beta \rightarrow \infty$, and it is not necessary to have the separate
 107 equalities $\gamma_1 = K_1$, $\gamma_2 = K_2$; the condition is only on the ratio: $\gamma_2/\gamma_1 = K_2/K_1$. Anyway,
 108 this special case is by no means a representative of the general case.

109 3 Influence of dispersal on total population size

110 In the previous section, we saw that, depending on the values of the migration param-
 111 eters β and γ_2/γ_1 , the equilibrium can be anywhere on the ellipse \mathcal{E} in the positive
 112 quadrant. In this section, we will describe how this position affects the total equi-
 113 librium population N_T^* of model (3). In particular, we will investigate whether N_T^* is
 114 greater or smaller than $K_1 + K_2$. The analysis can largely be done graphically.

115 On Fig. 3, the straight line Δ is the line of slope -1 passing through the point
 116 $A = (K_1, K_2)$. It is the set of points with $N_1 + N_2 = K_1 + K_2$. For any equilibrium
 117 $E = (N_1^*, N_2^*)$, the total population $N_T^* = N_1^* + N_2^*$ can be read on the intersection with
 118 the horizontal axis of the straight line of slope -1 passing through E . We see very

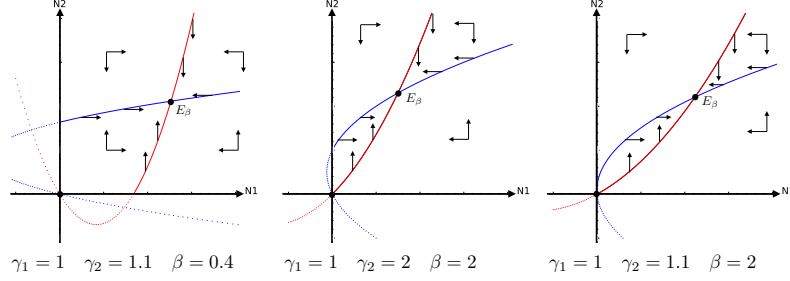


Figure 2: The isoclines of (3) are drawn (in red for N_1 , in blue for N_2) for the parameter values $r_1 = 1, r_2 = 2, K_1 = 1.4, K_2 = 2$ and for three different combinations of migration parameters. These three examples are typical of all possible configurations. In all cases the trajectories are attracted by E_β .

119 simply that dispersal is favorable to N_T^* if E is above Δ , unfavorable if below Δ . For
 120 example, on Fig. 3, dispersal is favorable when the equilibrium is E_{β_1} and unfavorable
 121 when the equilibrium is E_{β_2} .

122 Let us consider the slope of the ellipse \mathcal{E} at point $A = (K_1, K_2)$. By differentiating
 123 the ellipse equation (5) with respect to N_1 , it is easy to calculate that this slope is equal
 124 to $-r_1/r_2$.

125 In the special case $r_1 = r_2$, the slope is precisely -1 , which means that the ellipse
 126 \mathcal{E} is entirely below the straight line Δ except for the point A , which is exactly on Δ .
 127 This result can be stated as the following proposition:

128 **Proposition 1** *If $r_1 = r_2$, dispersal is always unfavorable to N_T^* .*

129 When $r_1 \neq r_2$, we will assume, with no loss of generality, that $r_1 < r_2$ (as in Fig.
 130 3). In this case, the point A is still an intersection of \mathcal{E} with Δ but there exists a second
 131 intersection point, which we denote by C (see Fig. 3).

132 We denote by Σ the straight line joining the origin to C and by σ the slope of Σ . An
 133 easy calculation shows that the coordinates of C are:

$$C = \left(\frac{r_2 K_1 (K_1 + K_2)}{r_1 K_2 + r_2 K_1}, \frac{r_1 K_2 (K_1 + K_2)}{r_1 K_2 + r_2 K_1} \right), \quad (8)$$

134 meaning that the slope σ is:

$$\sigma = \frac{r_1 K_2}{r_2 K_1}. \quad (9)$$

135 The rest of this section is essentially a comment of Figs. 4 and 5. We saw in Section
 136 2 that the equilibrium E_β follows the ellipse arc AB when β varies from 0 to ∞ , where
 137 B is the intersection of the ellipse \mathcal{E} with the oblique line \mathcal{P}_∞ . Since the slope of \mathcal{P}_∞

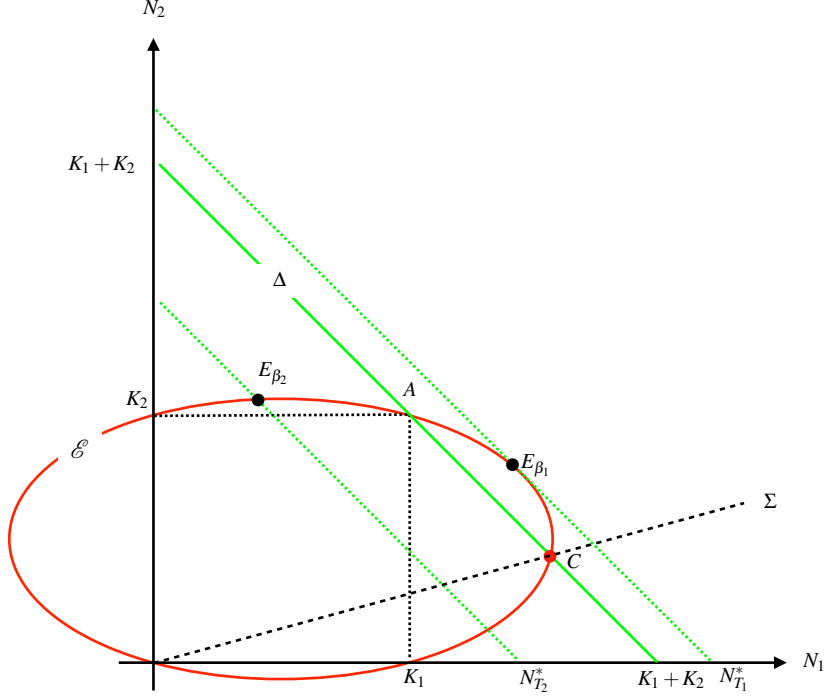


Figure 3: The straight line Δ is the set of points with $N_1 + N_2 = K_1 + K_2$. E_{β_1} is an example equilibrium point for which dispersal is favorable, while E_{β_2} is an example of unfavorable dispersal.

is γ_2/γ_1 , we will distinguish the following three cases, as this slope increases:

$$(a) \quad \frac{\gamma_2}{\gamma_1} < \frac{r_1 K_2}{r_2 K_1}, \quad (b) \quad \frac{r_1 K_2}{r_2 K_1} \leq \frac{\gamma_2}{\gamma_1} < \frac{K_2}{K_1}, \quad (c) \quad \frac{K_2}{K_1} \leq \frac{\gamma_2}{\gamma_1}. \quad (10)$$

Figure 4 presents the case (a), in which \mathcal{P}_∞ is lower than Σ . Figure 5 presents the other two cases, with \mathcal{P}_∞ higher than Σ but lower than A (case b) and \mathcal{P}_∞ higher than A (case c). Besides each of the pictures in the state space $N_1 \times N_2$, we show a qualitative graph of the function $\beta \mapsto N_T^*(\beta)$.

Let us first consider the case (a) on Fig. 4. For $\beta = 0$, the equilibrium point starts at A and, as β increases, E_β moves clockwise along \mathcal{E} and ends at B . The total equilibrium population $N_T^*(\beta)$ starts with the value $K_1 + K_2$ at A , then increases, attains a maximum N_{max}^* for some β_{max} , decreases to $K_1 + K_2$ again at point C for some β_C and decreases further to the limit corresponding to point B . Note that N_{max}^* , β_{max} , β_C , and B can all be calculated explicitly but we will not give them here because the expressions are heavy and have no practical interest.

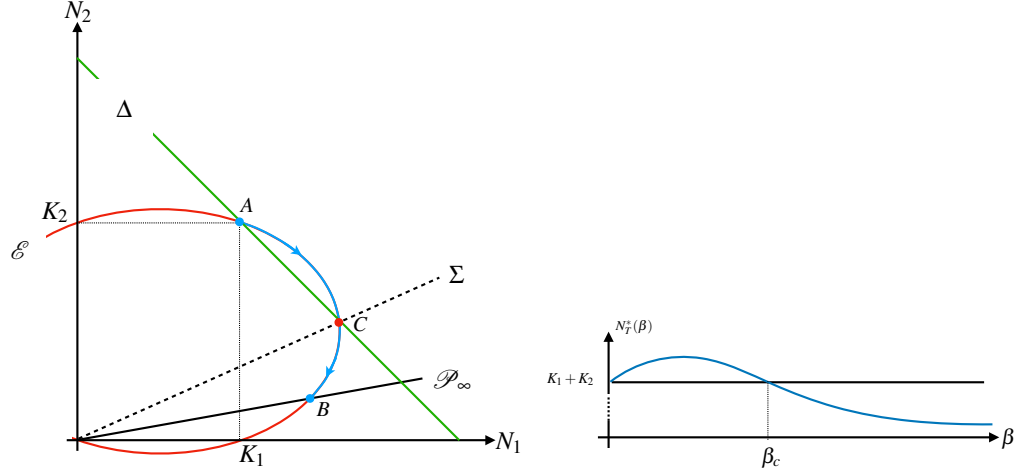


Figure 4: This illustrates the case (a) of (10). As the migration intensity β increases from 0 to ∞ , the equilibrium point moves clockwise along the ellipse \mathcal{E} from A to B, passing through C.

For the other two cases (Fig. 5), descriptions are similar but simpler because $N_T^*(\beta)$ is either always greater than $K_1 + K_2$ (case b) or always smaller than $K_1 + K_2$ (case c). This description can be summarized in the following proposition.

Proposition 2 Assume that $r_1 < r_2$. Then:

- (a) $\frac{\gamma_2}{\gamma_1} < \frac{r_1 K_2}{r_2 K_1} \implies$ there exists β_c such that
 - $0 \leq \beta \leq \beta_c \implies N_T^*(\beta) \geq K_1 + K_2,$
 - $\beta_c < \beta \implies N_T^*(\beta) < K_1 + K_2,$
- (b) $\frac{r_1 K_2}{r_2 K_1} \leq \frac{\gamma_2}{\gamma_1} < \frac{K_2}{K_1} \implies N_T^*(\beta) \geq K_1 + K_2$ for every β ,
- (c) $\frac{K_2}{K_1} \leq \frac{\gamma_2}{\gamma_1} \implies N_T^*(\beta) \leq K_1 + K_2$ for every β .

4 Discussion

The ecological problem that has motivated this study is to find the conditions for which fragmentation and dispersal can lead to higher total equilibrium population abundance N_T^* than the sum $K_1 + K_2$. Mathematically, this is the six-parameter problem posed by model (3) that we have solved in the present paper.

The propositions 1 and 2 contain the full set of results of the present general model (3). They show that all parameters have an influence in determining whether N_T^* is

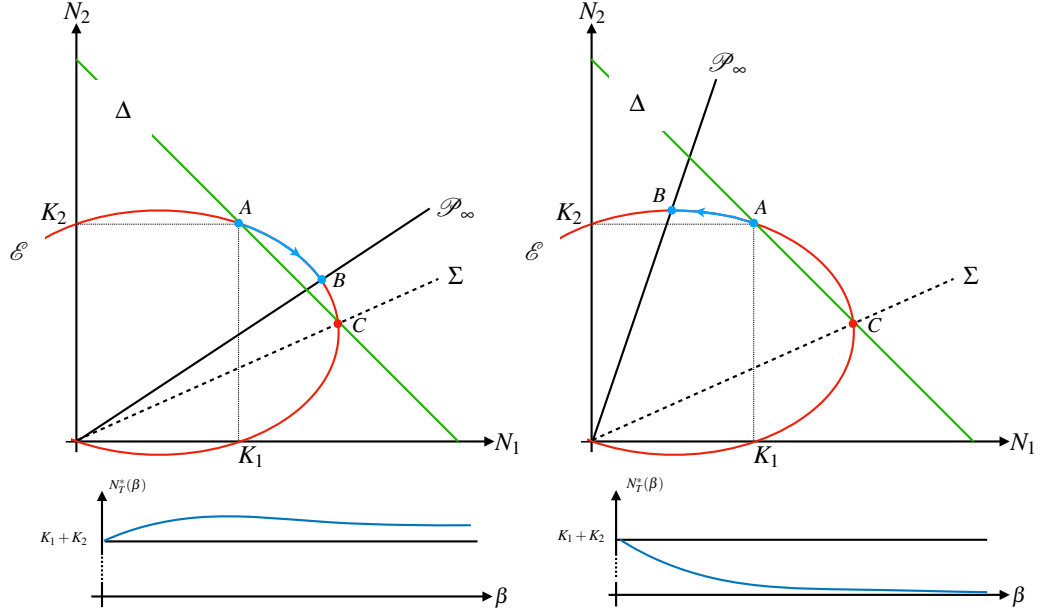


Figure 5: Left: case (b) of (10). As the equilibrium point moves clockwise from A to B with increasing β , it is always greater than $K_1 + K_2$. Right: case (c) of (10). As the equilibrium point moves counterclockwise from A to B with increasing β , it is always smaller than $K_1 + K_2$.

higher or lower than $K_1 + K_2$. Compared with earlier models, which new results are brought by dispersal asymmetry? This can be found by investigating the influence of γ_2/γ_1 in the two propositions, and by considering the special value $\gamma_2/\gamma_1 = 1$ that corresponds to symmetric dispersal.

Proposition 1 does not depend on γ_2/γ_1 and remains valid in the case of symmetric dispersal: dispersal is always unfavorable when $r_1 = r_2$.

In Proposition 2 for $r_1 < r_2$, the assumption of symmetric dispersal simplifies the conditions for the three cases, which become:

$$(a) \quad 1 < \frac{r_1}{r_2} \frac{K_2}{K_1}, \quad (b) \quad \frac{r_1}{r_2} \frac{K_2}{K_1} \leq 1 < \frac{K_2}{K_1}, \quad (c) \quad \frac{K_2}{K_1} \leq 1. \quad (11)$$

As an example, let us have a closer look at condition (c). If this condition is satisfied, dispersal always has an unfavorable effect on total abundance, for any dispersal intensity β . If dispersal is symmetric, the inequality (11c) means that (with $r_1 < r_2$), the total equilibrium abundance N_T^* will always be lower than $K_1 + K_2$ when $K_2 \leq K_1$. However, in the presence of dispersal asymmetry, the corresponding condition (10c) is not necessarily satisfied: if the asymmetry is such that $\gamma_2/\gamma_1 \ll 1$, dispersal can become favorable. Conversely, if $\gamma_2/\gamma_1 \gg 1$, dispersal remains unfavorable in wider conditions

181 of the ratio K_2/K_1 . Similarly, the conditions (10a) and (10b) are also influenced by the
 182 asymmetry γ_2/γ_1 .

183 In sum, dispersal asymmetry can play a crucial role. The various patterns describ-
 184 ing the influence of dispersal on total population abundance (the small graphs in Figs. 4
 185 and 5) remain qualitatively the same whether dispersal is symmetric or not. However,
 186 comparing the conditions (10) and (11) shows that dispersal asymmetry can have a
 187 strong quantitative influence, depending on its magnitude and on its direction. In com-
 188 bination with the other parameters, it can either amplify or attenuate the favorable or
 189 unfavorable effects of dispersal intensity. Strong asymmetry combined with high dis-
 190 persal intensity can reverse the predictions of symmetric dispersal. This is particularly
 191 important if the model is used for applied purposes such as population conservation or
 192 pest control.

References

- [1] Arditi, R., Bersier, L.F., Rohr, R.P., 2016. The perfect mixing paradox and the logistic equation: Verhulst vs. Lotka. *Ecosphere* 7(11):e01599.
- [2] Arditi, R., Bersier, L.F., Rohr, R.P., 2017. The perfect mixing paradox and the logistic equation: Verhulst vs. Lotka: Reply. *Ecosphere* 8(7):e01894.
- [3] Arditi, R., Lobry, C., Sari, T., 2015. Is dispersal always beneficial to carrying capacity? New insights from the multi-patch logistic equation. *Theoretical Population Biology* 106, 45–59.
- [4] DeAngelis, D.L., Ni, W.M., Zhang, B., 2016. Effects of dispersal in a non-uniform environment on population dynamics and competition: a patch model approach. *Theoretical Ecology* 9, 443–453.
- [5] DeAngelis, D.L., Travis, C.C., Post, W.M., 1979. Persistence and stability of seed-dispersed species in a patchy environment. *Theoretical Population Biology* 16, 107–125. doi:10.1016/0040-5809(79)90008-X.
- [6] DeAngelis, D.L., Zhang, B., 2014. Effects of diffusion on total biomass in heterogeneous continuous and discrete-patch systems. *Discrete and Continuous Dynamical Systems Series B* 19, 3087–3104. doi:10.3934/dcdsb.2014.19.3087.
- [7] Freedman, H.I., Waltman, D., 1977. Mathematical models of population interactions with dispersal. I. Stability of two habitats with and without a predator. *SIAM Journal of Applied Mathematics* 32, 631–648. doi:10.1137/0132052.
- [8] Hanski, I., 1999. *Metapopulation Ecology*. Oxford University Press.
- [9] Holt, R.D., 1985. Population dynamics in two-patch environments: Some anomalous consequences of an optimal habitat distribution. *Theoretical Population Biology* 28, 181–208. doi:10.1016/0040-5809(85)90027-9.
- [10] Ramos-Jiliberto, R., Moisset de Espanés, P., 2017. The perfect mixing paradox and the logistic equation: Verhulst vs. Lotka: Comment. *Ecosphere* 8:e01895.